COMPUTATIONAL MECHANICS 2023
38th conference with international participation
Srní
October 23 - 25, 2023

Modelling of pulse-triggered running waves on a blade cascade

P. Šnábl[a], L. Pešek[a]

[a] *Institute of Thermomechanics of the CAS, v. v. i., Dolejškova 1402/5, 182 00 Praha 8, Czech Republic*

An experimental cascade of five NACA 0010 blades with pitch degrees of freedom is excited by a moment pulse to one of the blades. Depending on the flow conditions, such as wind speed and the angle of attack of the wind on the blades, the vibration of the excited blade is transmitted by the wind to the other blades. This can result in a running wave that diminishes over time or in a flutter running wave.

A simplified spring-mass-damper model with inter-blade connections and non-linear van der Pol dampers is tuned to match experimentally obtained stability curves and tested to see if it can qualitatively model the response of the cascade to the pulse excitation.

The motion equations of all five blades with inertia $\mathbf{I}$, damping $\mathbf{B}$ and stiffness $\mathbf{K}$ and blade displacement $\boldsymbol{\varphi}$ can be written as

$$\mathbf{I}\ddot{\boldsymbol{\varphi}} + \mathbf{B}\dot{\boldsymbol{\varphi}} + \mathbf{K}\boldsymbol{\varphi} + \mathbf{g}(\boldsymbol{\varphi},\ \dot{\boldsymbol{\varphi}}) = \mathbf{m_E}, \tag{1}$$

where the additional nonlinear term $\mathbf{g}(\boldsymbol{\varphi},\ \dot{\boldsymbol{\varphi}})$ describes the aeroelastic couplings between the blades and the right-hand vector $\mathbf{m_E}$ adds the moment of the pulse excitation.

The question is how to mathematically describe the complex fluid-structure interaction that is present in the experimental blade cascade. In our previous works, e.g., [1], we used the van der Pol damping term, which can be written for the pitch motion of the blade i as

$$g_i(\boldsymbol{\varphi},\ \dot{\boldsymbol{\varphi}}) = -\mu\left[1 - \left(\frac{\varphi_i}{r}\right)^2\right]\dot{\varphi}_i. \tag{2}$$

It is a negative damping with an intensity μ that becomes positive when the displacement of the blade exceeds the threshold value set by r. This change of sign causes excitation of the blades at low amplitudes and damping at high amplitudes which is advantageous in simulations because the amplitudes do not grow to infinity. It also corresponds to the experiment with only one blade installed - at certain flow conditions the blade starts to self-oscillate, but after a short transition period the amplitude settles at certain value. However, equation (2) for blade i does not contain any information about adjacent blades. Thus, each blade can oscillate independently which is not the case in experiment with multiple blades.

To interconnect the blades, the van der Pol damping equation (2) was modified in [2] to act on the relative motion of the adjacent blades

$$\begin{aligned} g_i(\boldsymbol{\varphi},\ \dot{\boldsymbol{\varphi}}) = -\mu_R\Bigg\{ &\left[1 - \left(\frac{\varphi_i - \varphi_{i-1}}{r_R}\right)^2\right](\dot{\varphi}_i - \dot{\varphi}_{i-1}) + \\ &+ \left[1 - \left(\frac{\varphi_i - \varphi_{i+1}}{r_R}\right)^2\right](\dot{\varphi}_i - \dot{\varphi}_{i+1})\Bigg\}. \end{aligned} \tag{3}$$

Equation (3) reaches a minimal value when the adjacent blades oscillate in opposite phase, at an inter-blade phase angle (IBPA) of 180°, which forces the blades to oscillate at this IBPA. However, this is not the case in our experiments.

This is shown graphically in Fig. 1 where the aerodynamic damping (AD) parameter, which corresponds to the work done by the moment acting on the blade during one period of blade motion, is plotted as a function of IBPA. Negative AD means that the moment is exciting the blade, positive AD means that the moment is damping the blade. While in the experiment the AD follows a typical so-called S-curve with a minimum around -90° and a maximum around 90°, the AD provided the by relative motion van der Pol damping from (3) together with the viscous damping term $\mathbf{B}\dot{\boldsymbol{\varphi}}$ from (1) actually shows a minimum at 180°.

The aim of this paper is to introduce such a term $\mathbf{g}(\boldsymbol{\varphi},\ \dot{\boldsymbol{\varphi}})$ that would add damping to the system corresponding to the experiment. The suggested term for the blade i is

$$g_i(\boldsymbol{\varphi}) = k_{AE}\left[r_1 r_2 \varphi_{i-1} + (r_2^2 - r_1^2)\varphi_i - r_1 r_2 \varphi_{i+1}\right]. \tag{4}$$

This equation is based on a virtual spring attached between the i-th blade trailing edge at arm r_1 from the blade axis and the $(i+1)$-th blade leading edge at arm r_2 from the blade axis. However, this would only create an elastic connection with no ability to damp or excite the system. Therefore, the sign of the virtual spring force acting on the trailing edge of each blade was reversed, resulting in a non-conservative force. Equation (4) can then be tuned to match the experimentally obtained S-curve with the aeroelastic "stiffness" parameter k_{AE}, as shown in Fig. 2. The values of the arm lengths are set according to the blade cascade geometry: $r_1 > r_2$.

Both the experimental and numerical S-curves in Fig. 2 were obtained using the travelling wave mode approach with a blade oscillation amplitude of 1° and frequency of 25 Hz. The experiment was carried out at a wind speed of 25 m/s and an angle of attack of $-8°$ (negative sign corresponds to the turbine configuration).

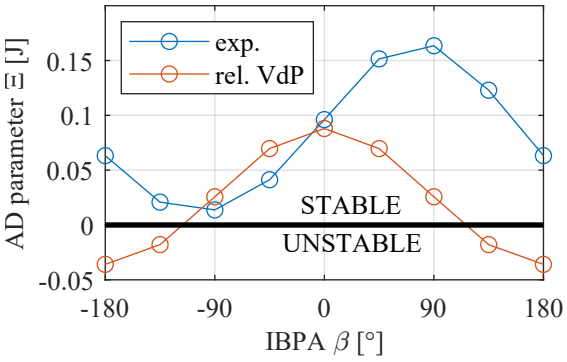

Fig. 1. Experimentally measured aerodynamic damping in comparison with simulated aerodynamic damping using relative motion van der Pol damping equation

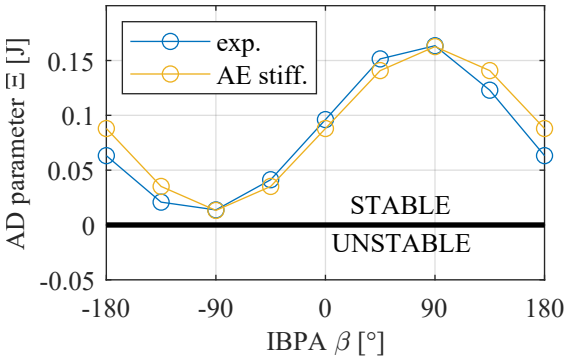

Fig. 2. Experimentally measured aerodynamic damping in comparison with simulated aerodynamic damping using herein proposed aeroelastic stiffness

The next step is to simulate the behaviour of the blade cascade behaviour when one of the blades is excited by a moment pulse. This was done experimentally with the first and last blade fixed. The experimental results are shown in Figs. 3a, 4a and 5a, where the pulse was applied to the blades $+1$, 0 and -1, respectively. The displacement of all three non-fixed blades can be observed and the most important is the IBPA between the blades. It can be seen that in all three cases the blade $+1$ is followed by blade 0 and blade 0 is followed by blade -1. This means that a backward running wave was excited which is consistent with the S-curve in Figs. 1 and 2,

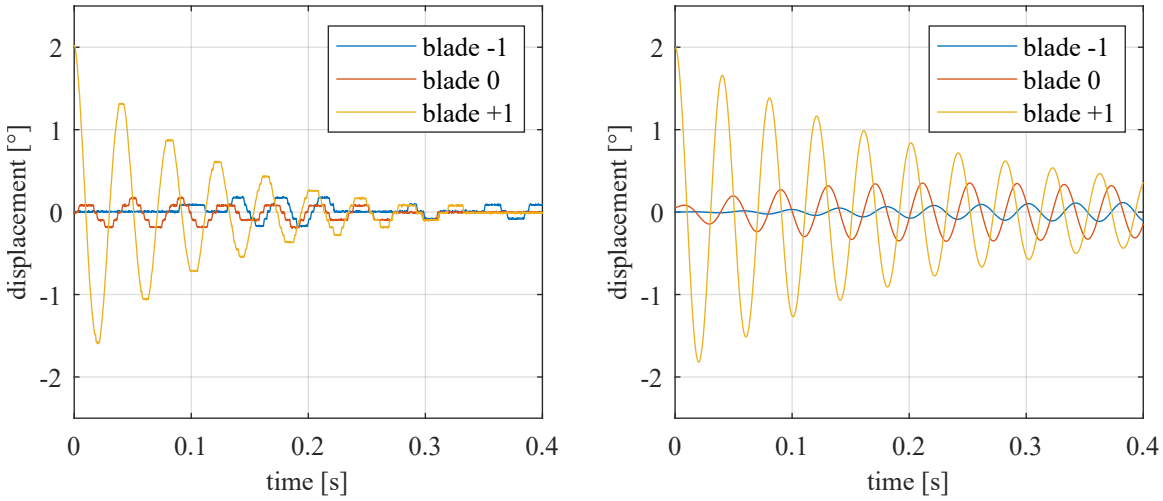

(a) Experiment (25 m/s, AOA $-8°$) (b) Simulation

Fig. 3. Behaviour of the blade cascade after pulse excitation of the blade $+1$

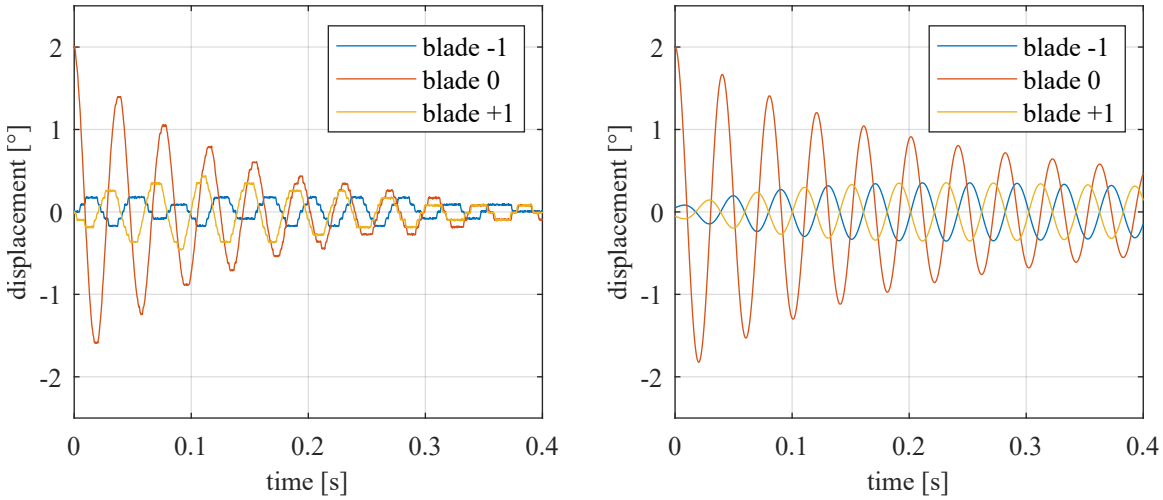

(a) Experiment (25 m/s, AOA $-8°$) (b) Simulation

Fig. 4. Behaviour of the blade cascade after pulse excitation of the blade 0

where negative IBPA corresponds to the backward running wave. The minimal AD is at IBPA $-90°$ and this is the most likely phase angle at which the blade cascade starts to oscillate.

Simulations of the system described by (1) with the aeroelastic term (4) tuned to match the experimental S-curve as shown in Fig. 2 were carried out in Simulink and the results are shown in Figs. 3b, 4b and 5b with pulses to the blades $+1$, 0 and -1, respectively.

With the pulse applied to the blades $+1$ and 0 in Figs. 3 and 4, we can see qualitatively very similar behaviour in the experiment and simulation. After the pulse, the adjacent blades start to oscillate, creating the backward running wave. In the simulation the IBPA is always $-90°$. However, in the experiment this is not always true, e.g., in Fig. 4a the IBPA of the blade -1 with respect to the blade 0 is somewhere in between $0°$ and $-90°$. There is also a noticeable difference in the overall damping. Although the damping in simulation is also tuned to match the experimental S-curve, the oscillations decay faster in the experiment than in the simulation.

A different scenario can be seen when the pulse is applied to the blade -1 in Fig. 5. While the simulation behaves similarly to the previous cases and in accordance with the S-curve in

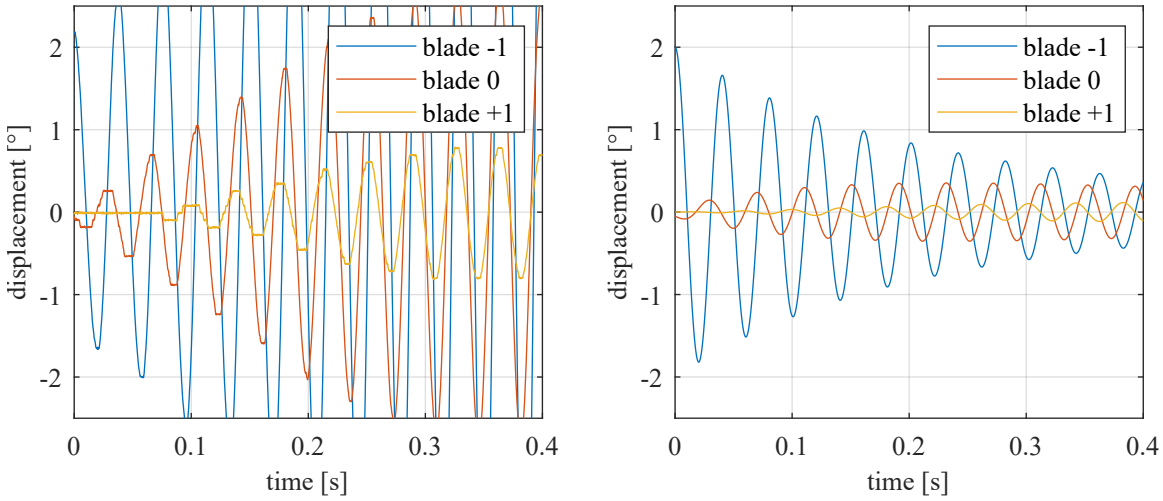

(a) Experiment (25 m/s, AOA $-8°$)

(b) Simulation

Fig. 5. Behaviour of the blade cascade after pulse excitation of the blade -1

Fig. 2 where the AD is always positive and no self-excitation should occur, the reality in the experiment is different. After the pulse in Fig. 5b we can see the onset of the cascade flutter with diverging amplitudes of all the blades.

It must be noted that the case at 25 m/s and AOA $-8°$ is right at the flutter boundary. At AOA $-7°$ the flutter does not start after the pulse to the blade -1, at AOA $-9°$ the cascade starts to flutter even without any pulse. Also, at AOA $-8°$ the flutter will not start if the pulse to the blade -1 is smaller.

Although the cascade model with the proposed aeroelastic term (4) could not capture the onset of the flutter, which is understandable due to the enormous complexity of the fluid-structure interaction, it was able to very realistically interconnect the blades and simulate the blade cascade behaviour in non-flutter regimes which is a great achievement. To simulate the rapid increase in amplitudes when the flutter occurs, another term in the motion equations is needed, possibly a variant of the van der Pol damping equation. Further experiments and simulations will be carried out in the future to model the aeroelastic coupling even more accurately and possibly even capture the flutter behaviour.

Acknowledgement

This work was supported by the conceptual development project RVO: 61388998 of the Institute of Thermomechanics of the CAS, v. v. i.

References

[1] Pešek, L., Šnábl, P., Prasad, C. S., Modal synthesis method for inter-blade dry-friction surface angle design of turbine wheel for vibration suppression, Proceedings of the ASME 2022 International Design Engineering Technical Conferences and Computers and Information in Engineering Conference, 2022, V010T10A022.

[2] Pešek, L., Šnábl, P., Prasad, C. S., Delanney, Y., Numerical simulations of aeroelastic instabilities in turbine-blade cascade by a modified Van der Pol model at running excitation, Applied and Computational Mechanics 17 (1) (2023) 35-52.